BIOCHEMISTRY
including biophysical chemistry & molecular biology

Article

pubs.acs.org/biochemistry

Biochemical and Kinetic Characterization of Radical *S*-Adenosyl-L-methionine Enzyme HydG

Rebecca C. Driesener,[†] Benjamin R. Duffus,[‡] Eric M. Shepard,[‡] Ian R. Bruzas,[‡] Kaitlin S. Duschene,[‡] Natalie J.-R. Coleman,[†] Alexander P. G. Marrison,[†] Enrico Salvadori,[§,∥] Christopher W. M. Kay,[§,∥] John W. Peters,[‡] Joan B. Broderick,[‡] and Peter L. Roach*[,†,⊥]

[†]Chemistry, Faculty of Natural and Engineering Sciences, University of Southampton, Highfield SO17 1BJ, U.K.
[‡]Department of Chemistry and Biochemistry, Montana State University, Bozeman, Montana 59717, United States
[§]Institute of Structural and Molecular Biology, University College London, Gower Street, London WC1E 6BT, U.K.
[∥]London Centre for Nanotechnology, University College London, 17-19 Gordon Street, London WC1H 0AH, U.K.
[⊥]Institute for Life Sciences, University of Southampton, Highfield SO17 1BJ, U.K.

Supporting Information

ABSTRACT: The radical *S*-adenosyl-L-methionine (AdoMet) enzyme HydG is one of three maturase enzymes involved in [FeFe]-hydrogenase H-cluster assembly. It catalyzes L-tyrosine cleavage to yield the H-cluster cyanide and carbon monoxide ligands as well as *p*-cresol. *Clostridium acetobutylicum* HydG contains the conserved CX_3CX_2C motif coordinating the AdoMet binding [4Fe-4S] cluster and a C-terminal $CX_2CX_{22}C$ motif proposed to coordinate a second [4Fe-4S] cluster. To improve our understanding of the roles of each of these iron−sulfur clusters in catalysis, we have generated HydG variants lacking either the N- or C-terminal cluster and examined these using spectroscopic and kinetic methods. We have used iron analyses, UV−visible spectroscopy, and electron paramagnetic resonance (EPR) spectroscopy of an N-terminal C96/100/103A triple HydG mutant that cannot coordinate the radical AdoMet cluster to unambiguously show that the C-terminal cysteine motif coordinates an auxiliary [4Fe-4S] cluster. Spectroscopic comparison with a C-terminally truncated HydG (ΔCTD) harboring only the N-terminal cluster demonstrates that both clusters have similar UV−visible and EPR spectral properties, but that AdoMet binding and cleavage occur only at the N-terminal radical AdoMet cluster. To elucidate which steps in the catalytic cycle of HydG require the auxiliary [4Fe-4S] cluster, we compared the Michaelis−Menten constants for AdoMet and L-tyrosine for reconstituted wild-type, C386S, and ΔCTD HydG and demonstrate that these C-terminal modifications do not affect the affinity for AdoMet but that the affinity for L-tyrosine is drastically reduced compared to that of wild-type HydG. Further detailed kinetic characterization of these HydG mutants demonstrates that the C-terminal cluster and residues are not essential for L-tyrosine cleavage to *p*-cresol but are necessary for conversion of a tyrosine-derived intermediate to cyanide and CO.

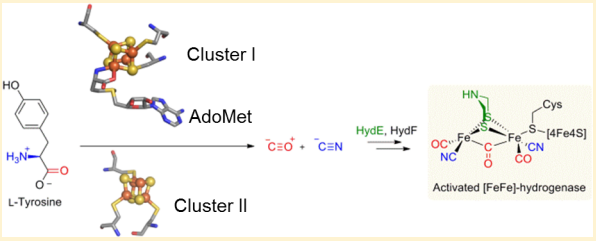

Hydrogenases catalyze the efficient formation of molecular hydrogen through reduction of protons. Three phylogenetically unrelated hydrogenase classes can be distinguished on the basis of their active site metal content: [FeFe]-, [NiFe]-, and [Fe]-hydrogenases.[1,2] The [FeFe]-hydrogenase cofactor consists of a [4Fe-4S] cluster bridged to a [2Fe] subcluster containing CO and cyanide ligands[3,4] as well as a bis-(thiomethyl)amine bridge[5−7] (Scheme 1). Recent evidence indicates that the cofactor is assembled in a stepwise process,[8] where the loaded [2Fe] subcluster is transferred from HydF to the [FeFe]-hydrogenase protein already containing the [4Fe-4S] cluster.[8,9] The demonstration that purified *Clostridium acetobutylicum* (*Ca*) HydF heterologously expressed in the background of *Ca* HydE and *Ca* HydG ($HydF^{EG}$) is sufficient to activate the [FeFe]-hydrogenase from *Clostridium pasteurianum* (*CpI*) heterologously expressed in the absence of the maturases led to the proposal of HydF as a scaffold protein.[10] This was supported by the observation of cluster-bound cyanide and CO ligands in the Fourier transform infrared (FTIR) spectrum of $HydF^{EG}$.[11,12] The demonstration that *Desulfovibrio vulgaris* HydF does not interact with its putative [FeFe]-hydrogenase[13] implies that the proposed action of HydF as a scaffold for H-cluster synthesis might not be strictly conserved. Similarly, *Shewanella oneidensis* HydG was the only maturase necessary for *CpI* [FeFe]-hydrogenase activation in the presence of a desalted *Escherichia coli* lysate and additional small molecule substrates like L-tyrosine (tyrosine hereafter) and AdoMet,[14] suggesting that HydG might be acting as a scaffold protein. HydG has been shown to cleave tyrosine to produce *p*-cresol,[15] cyanide,[16] and CO.[17] Evidence that the

Received: August 20, 2013
Revised: November 6, 2013
Published: November 8, 2013

Scheme 1. Role of HydG in [FeFe]-Hydrogenase Cofactor Assembly

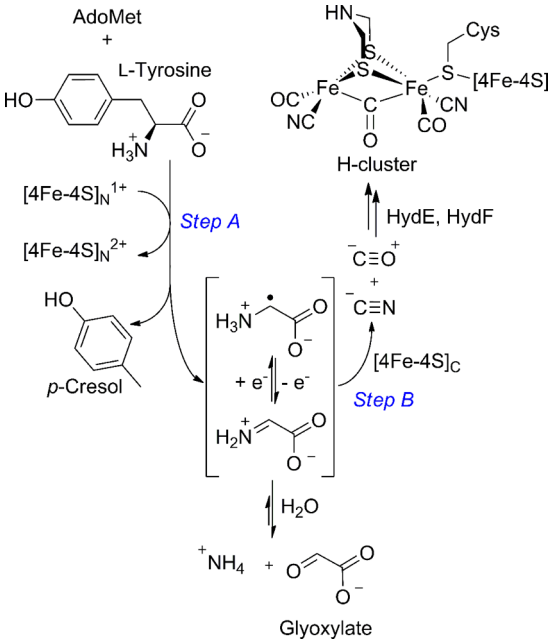

diatomic molecules are incorporated into the H-cluster came from characteristic shifts in the vibrational cyanide and CO energies of the *CpI* [FeFe]-hydrogenase produced *in vitro* with natural abundance or isotopically labeled tyrosine.[18] HydE has been proposed to have a role in the biosynthesis of the dithiolate bridge[12] or translocation of the [2Fe] subcluster,[14] but despite the availability of the crystal structure of HydE,[19] the substrate still needs to be identified. Even with more information about [FeFe]-hydrogenase cofactor assembly and transfer becoming available, detailed mechanistic insights into HydG-based cyanide and CO ligand synthesis are lacking.

HydG and HydE both belong to the radical AdoMet superfamily of enzymes,[20] which was initially characterized by a conserved N-terminal CX_3CX_2C motif[21] and the requirement for a reduced $[4Fe\text{-}4S]^+$ cluster and AdoMet for activity.[22] Three iron atoms of this [4Fe-4S] cluster (cluster I) are coordinated by the conserved cysteines, whereas the fourth, unique iron is coordinated by the α-amino and α-carboxy groups of AdoMet.[23−26] The transfer of a single electron from the cluster to AdoMet initiates homolytic C−S bond cleavage,[27] generating a highly reactive 5′-deoxyadenosyl radical.[28,29] This radical in turn abstracts a hydrogen atom from the substrate to generate a substrate radical, which undergoes further rearrangement or cleavage to the final product(s).

Sequence analyses suggest that HydG belongs to a subclass of radical AdoMet enzymes that act on amino acids during cofactor biosynthesis[16,30] and include tyrosine lyase (ThiH) for anaerobic thiamine biosynthesis,[31−33] NocL and NosL for nosiheptide biosynthesis,[34,35] and FbiC (CofG/CofH in cyanobacteria) for the biosynthesis of the F_{420} cofactor.[30] The sequence of HydG is 27% identical with that of ThiH,[15] and under anaerobic conditions, both cleave the $C_\alpha-C_\beta$ bond of tyrosine in an AdoMet-dependent manner to yield *p*-cresol.[15,32] An energetically more favored homolytic cleavage reaction yields a C-centered glycine radical as the nonaromatic intermediate, while heterolytic cleavage results in the formation of dehydroglycine[32] (Scheme 1). During the turnover of ThiH, glyoxylate accumulates and is presumed to be the product of dehydroglycine hydrolysis,[32] whereas little glyoxylate is formed during HydG catalysis.[16] Instead, stoichiometric quantities of cyanide[16] with respect to *p*-cresol were detected as well as substoichiometric amounts of CO.[17]

Initial spectroscopic characterization of chemically reconstituted *Thermotoga maritima* HydG indicated the presence of one and possibly two [4Fe-4S] clusters.[20] The primary sequence of *Ca* HydG contains two cysteine motifs that have both been shown to be essential for activation of the [FeFe]-hydrogenase.[36] While the radical AdoMet CX_3CX_2C triad at the N-terminus is well-conserved, the additional $CX_2CX_{22}C$ motif at the C-terminus, proposed to coordinate the second [4Fe-4S] cluster (cluster II),[36] displays some variation.[37] For 301 HydG homologues investigated, only the first and last cysteine residue (C386 and C412, respectively, in the *Ca* HydG sequence) of the C-terminal motif were found to be conserved.[37] Clear evidence of the presence of an accessory [4Fe-4S] cluster II came from iron content analyses and EPR spectra of reconstituted *Ca* HydG in the absence and presence of AdoMet.[17]

Other radical AdoMet enzymes containing an auxiliary (mostly [4Fe-4S]) cluster have been identified and some studied in great detail.[38] The functional importance of the HydG auxiliary cluster II in cyanide synthesis was inferred in a mutagenesis study: approximately 50 and 100% decreases in the extent of cyanide formation were observed for a *Ca* HydG $SX_2SX_{22}C$ double mutant and a mutant lacking the entire C-terminal domain, including the cysteine motif (ΔCTD), respectively.[39] In the mechanistic proposal for HydG (Scheme 1), the reaction step being affected by these mutations could have been either tyrosine cleavage (step A) or the synthesis of cyanide and CO (step B). This question was addressed by further studies[40] in which *Thermoanaerobacter tengcongensis* (*Tte*) ΔCTD HydG was shown to have a tyrosine cleavage activity more than 98% reduced compared to that of the wild-type (WT) enzyme, forming only 0.04 molar equiv (1 μM) of *p*-cresol. These very low levels of *p*-cresol may indicate poor turnover of tyrosine, and this may explain the apparent absence of detected cyanide. The lack of CO formation and the decreased iron content of the $SX_2SX_{22}C$ and ΔCTD HydG variants compared to the values of the WT enzyme were rationalized by the proposal that cluster II is not required for cyanide but is essential for CO synthesis.[39] The proposal that the second cluster is required for the formation of a stable iron−carbonyl complex is consistent with the substoichiometric detection of CO formed by WT HydG.[17]

In this study, we prepared an N-terminal C96/100/103A mutant that cannot coordinate the radical AdoMet [4Fe-4S] cluster, a single C386S mutant, and a C-terminal deletion mutant. Characterization of WT HydG and these mutants by iron, UV−visible, and EPR spectral analyses supports a hypothesis in which the C-terminal $CX_2CX_{22}C$ motif coordinates an auxiliary [4Fe-4S] cluster II, which is unable to coordinate AdoMet. To establish the role of the auxiliary cluster II and C-terminal residues during tyrosine cleavage, the formation of *p*-cresol, cyanide, CO, and glyoxylate by WT HydG and C-terminal mutants has been compared. A prerequisite for these studies was the determination of the respective Michaelis−Menten constants for the AdoMet and tyrosine substrates. The Michaelis−Menten constants permitted the use of near-saturating substrate concentrations upon comparison of WT and mutant HydG enzymes, which in turn

dx.doi.org/10.1021/bi401143s | *Biochemistry* 2013, 52, 8696−8707

allowed us to assess the effect of mutations on the rate of reaction and on apparent substrate binding. Our results indicate that mutations affecting cluster II coordination are, at worst, mildly deleterious to the rate of reductive AdoMet cleavage and cleavage of tyrosine to *p*-cresol. Proteins lacking cluster II formed no detectable CO, highlighting the importance of the C-terminal cluster for CO formation.

MATERIALS AND METHODS

Except where otherwise stated, chemicals were reagent grade or better, purchased from commercial sources, and used without further purification. All solutions were prepared inside an anaerobic glovebox using deoxygenated buffers unless stated otherwise. Expression of *E. coli* AdoMet synthetase was conducted using overproducing strain DM22 (pK8) as described previously,[26] with slight modifications.[41] Enzymatically synthesized AdoMet was estimated by ^{1}H nuclear magnetic resonance to be 95% biologically active *S*,*S*-AdoMet and by HPLC analysis to contain <0.05% adenine and <1.5% 5′-methylthioadenosine and was used throughout these studies unless otherwise stated to prevent impurities in commercial AdoMet samples from inhibiting HydG.[42] The concentration of AdoMet was determined using its extinction coefficient (ε_{260}) of 15400 M^{-1} cm^{-1}.[43,44] Protein concentrations were determined using the Bradford assay[45] and bovine serum albumin as a standard. Tyrosine solutions were prepared by addition of a 25.7 mM stock in 200 mM HCl (350 μL) to 1 M NaOH (80 μL) and buffer D [50 mM Hepes and 0.5 M KCl (pH 7.4, 20 μL)], giving a 20 mM stock solution that was further diluted as needed.

Site-Directed Mutagenesis. Mutant genes *hydG_C96/100/103A*, *hydG_C386S*, and *hydG_ΔCTD* were prepared using a QuikChange Lightning Multi Site-Directed Mutagenesis Kit (Stratagene or Agilent Technologies, La Jolla, CA) using the *Ca hydG_WT* gene[10] as a template. Incorporation of the mutations and the absence of secondary mutations were confirmed by sequencing (Eurofins UK or Idaho State University Molecular Research Core Facility, Pocatello, ID).

Protein Expression, Purification, and Reconstitution. The pCDFDuet-1 plasmids encoding HydG variants from *C. acetobutylicum* were transformed into *E. coli* BL21(DE3) (Stratagene) and overexpressed as described previously,[17] with slight modifications. Briefly, single colonies obtained from transformations were grown overnight in LB medium and utilized to inoculate 9 L LB cultures containing 10 g/L tryptone, 5 g/L yeast extract, 5 g/L KCl, 5 g/L glucose, and 50 mM potassium phosphate buffer (pH 7.2). The cultures were grown at 37 °C while being shaken at 225 rpm until the OD_{600} reached 0.5, at which point 0.06 g/L ferrous ammonium sulfate (FAS) and isopropyl β-D-1-thiogalactopyranoside (final concentration of 1 mM) were added. The cultures were grown for an additional 2.5 h at 37 °C, at which time an additional aliquot of 0.06 g/L FAS was added. The cultures were then transferred to a 10 °C refrigerator and purged with N_2 overnight. Cells were harvested by centrifugation, and the resulting cell pellets were stored at −80 °C until further use. Protein expressions in Southampton were conducted as described previously,[16] but without the addition of FAS. Protein purifications were conducted as previously published[16] with the following modifications. Cell lysis was performed in the absence of PMSF, while sonication was achieved over five or six 10 min cycles of 1 s bursts (20 W). Buffer-exchanged protein fractions were pooled and concentrated to 30−40 mg/mL and flash-frozen in liquid N_2. Protein reconstitution was achieved by dropwise addition (over 20 min) of $FeCl_3$ followed by $Na_2S\cdot 9H_2O$ (10 equiv for WT and C386S HydG and 5 equiv for ΔCTD HydG) as 20 mM stock solutions in buffer C [20 mM Hepes, 0.5 M NaCl, 5% (w/v) glycerol, and 5 mM DTT (pH 7.4)] to protein solutions previously supplemented with DTT (5 mM). After the mixture had been gently stirred for 2 h, precipitated protein and excess iron sulfide were removed by centrifugation (SS-34, 13000 rpm, 4 °C, 20 min), and the protein was flash-frozen in liquid N_2 and stored as 0.5 mL aliquots at −80 °C until further use. Prior to experiments, proteins were freshly desalted into the required buffer via a pre-equilibrated PD-10 column packed with Sephadex G-25 (GE Healthcare). The efficiency of chemical reconstitution was then assessed by UV−visible spectroscopy and iron content analyses using the method of Fish.[46] Protein purification, reconstitutions, and assays performed in Montana followed previously published methods with slight modifications.[17]

EPR Spectroscopy. Reconstituted WT, C386S, and ΔCTD HydG proteins (~500 μM) in buffer C were thawed inside an anaerobic glovebox before being desalted into buffer D. Proteins were mixed with substrate(s) [1 mM commercial AdoMet, 1 mM *S*-adenosyl-L-homocysteine (AdoHcy), or 1 mM AdoHcy and 1 mM tyrosine] prepared in buffer D before the addition of sodium dithionite (1 mM). Following a 20 min incubation period, the mixture (160 μL) was transferred into an EPR tube (Wilmad Quartz, CFQ, 4 mm outside diameter) and sealed with a rubber septum before being flash-frozen in liquid N_2 outside the glovebox. EPR measurements at University College London (UCL) were performed on a Bruker EMXplus spectrometer operating at 9.4 GHz (X-band) equipped with a 4122SHQE resonator, with an Oxford Instruments ESR900 cryostat for measurements in the temperature range of 10−40 K. Measurements were performed with a magnetic field sweep from 0 to 600 mT, a microwave power of 2 mW, a modulation amplitude of 0.5 mT, and a modulation frequency of 100 kHz. EPR samples analyzed at Montana State University (MSU) were prepared as described previously.[17] Briefly, the HydG enzyme was supplemented with 50 mM Tris (pH 7.4), 100 μM deazariboflavin, and 5 mM DTT in buffer E [50 mM Hepes, 0.5 M KCl, and 5% (w/v) glycerol (pH 7.4)] and placed in an ice−water bath in the MBraun box. Following illumination with a 300 W Xe lamp for 1 h, enzymatically synthesized AdoMet (1 mM) was added in the absence of light. Within 3 min, the EPR tube was sealed with a rubber stopper and the sample flash-frozen in liquid N_2. Low-temperature EPR spectra were recorded using a Bruker (Billerica, MA) EMX X-band spectrometer equipped with a liquid helium cryostat and temperature controller from Oxford Instruments. Typical EPR parameters were as follows: sample temperature, 12 K; microwave frequency, 9.37 GHz; microwave power, 1.59 mW; time constant, 20.48 ms. Experimental spectra were baseline corrected and plotted using OriginLab (version 8.6.0, OriginLab Corp., Northampton, MA). All simulations of EPR data were performed using EasySpin[47] and yielded the *g* values reported throughout the text and summarized in the Supporting Information.

Determination of Michaelis−Menten Constants. Tyrosine cleavage was assessed by measuring initial rates of *p*-cresol formation as a function of AdoMet or tyrosine concentration. The AdoMet dependence was measured in assays (200 μL) containing reconstituted HydG (5 μM), tyrosine (400 μM for WT and 3 mM for C386S and ΔCTD

dx.doi.org/10.1021/bi401143s | *Biochemistry* 2013, 52, 8696−8707

HydG), sodium dithionite (1 mM), and varying concentrations of AdoMet (5−500 μM), while the dependence of the rate on tyrosine was determined in similar assays containing AdoMet (100 μM for WT and 200 μM for C386S and ΔCTD HydG) and varying concentrations of tyrosine (13 μM to 4 mM) instead. Control assays were devoid of sodium dithionite to accurately measure the nanomolar *p*-cresol impurities observed in tyrosine preparations. Assays were equilibrated at 37 °C for 5 min before initiation with sodium dithionite. Reactions were stopped at four time points between 1 and 14 min by addition of 20% perchloric acid (15 μL) and then mixtures stored at −80 °C before HPLC analysis. All assays were cleared by centrifugation (13000 rpm and 25 °C for 20 min) before the supernatant was analyzed for *p*-cresol using a modified HPLC procedure described by Challand et al.[33] In short, assay supernatants (40 μL) were applied to a Gemini C_{18} reverse phase HPLC column (4.6 mm × 250 mm, 5 μm, 110 Å, Phenomenex) equilibrated with 70% solvent A [0.1% (v/v) acetic acid in water, 0.8 mL/min]. After injection, the column was eluted for 5 min with 70% solvent A, followed by a gradient to 40% solvent B [0.1% (v/v) acetic acid in acetonitrile] over 3 min. An additional gradient over 7 min to 42% solvent B was applied before a step to 100% solvent B over 1 min where it was held isocratically for 8 min and then returned to 70% solvent A over 1 min. Before the next injection, the column was re-equilibrated with 70% solvent A for 5 min (total sampling time of 30 min). The fluorescence detector (Shimadzu RF-10Axl) measured excitation and emission at 274 and 312 nm, respectively. The amount of *p*-cresol (t_R = 15.9 min) was quantified using a calibration curve of synthetic standards (7.8−125 nM) analyzed in parallel. The quantification limit was 15 nM.

***In Vitro* Activity Assays.** Time course assays with all HydG variants contained reconstituted HydG (40 μM), AdoMet (0.5 mM), and tyrosine (4 mM) and were initiated with sodium dithionite (1 mM) as described above. Negative control assays were devoid of tyrosine. Duplicate reactions were stopped (1−60 min) by addition of 20% perchloric acid (15 μL), and then mixtures were immediately buffered by addition of 0.5 M Hepes (pH 7.5, 20 μL) and 1 M NaOH (30 μL) before being stored at −80 °C. HPLC analysis for 5′-deoxyadenosine (5′-dAH) and *p*-cresol was conducted as previously described.[16] Formed cyanide was quantified as the fluorescent 1-cyanobenz-[*f*]isoindole derivative with slight modifications.[16] Briefly, a solution to be analyzed (10 μL) was added to a freshly prepared working solution of MeOH, 20% NH_3, and 83 mM taurine in water (9:1:3, 65 μL) before addition of naphthalene-2,3-dicarboxaldehyde (10 mM in MeOH, 25 μL). After being incubated for 30 min at 20 °C, the solution was diluted 1:1 with water and immediately injected (40 μL) onto a pre-equilibrated HyperClone BDS C_{18} reverse phase HPLC column (4.6 mm × 150 mm, 5 μm, 130 Å, Phenomenex, 0.8 mL/min) for the most accurate results. Following sample injection, the column was eluted isocratically for 5 min using 60% solvent A (2 mM ammonium formate buffered to pH 3 with formic acid), before a gradient to 100% solvent B (MeOH) over 10 min was applied and then held isocratically for 10 min. The gradient was reversed to 60% solvent A over 1 min before the column was re-equilibrated for 9 min (total sampling time of 35 min). Under these conditions, the fluorescent 1-cyanobenz[*f*]-isoindole eluted with a t_R of 11.9 min (λ_{ex} = 418 nm; λ_{em} = 454 nm). Cyanide recovery in the presence of protein is reduced,[48] while sodium dithionite affects the fluorescence of the cyanide derivatization product. To accurately quantify cyanide, a calibration curve under assay conditions was employed where duplicate KCN standards (final concentrations of 1.25−160 μM) in 2.5 mM NaOH were added (80 μL) to activity assays (200 μL) lacking AdoMet and tyrosine. These assays were incubated for 12 and 38 min before being subjected to the precipitation−derivatization conditions described above. Glyoxylate was quantified as the fluoresecent 2-quinoxalinol derivative using a previously described method,[32] with slight modifications. Briefly, cleared assay supernatants (10 μL) were diluted with 50 mM Hepes (pH 7.5) to 50 μL before being acidified with 0.5 M HCl (100 μL) and addition of freshly prepared *o*-phenylene diamine in 0.5 M HCl (10 mg/mL, 50 μL). Using a polymerase chain reaction machine, all samples were incubated at 25 °C for 1 min, before being heated at 95 °C for 10 min and then cooled to 25 °C for 10 min before addition of 1.25 M NaOH (120 μL). After a 5 min period at 4 °C, the samples were stored at −80 °C and thawed only shortly before HPLC analysis. The derivatization mixture (40 μL) was injected onto an equilibrated HyperClone BDS C_{18} reverse phase HPLC column (4.6 mm × 150 mm, 5 μm, 130 Å, Phenomenex) connected to a fluorimeter (λ_{ex} = 350 nm; λ_{em} = 420 nm), and the column was washed with 85% solvent A (100 mM ammonium bicarbonate, 0.8 mL/min) for 5 min, followed by a gradient to 50% solvent B (acetonitrile) over 15 min. The gradient was increased to 100% solvent B over 1 min, held isocratically for 4 min, and returned to 85% solvent A over 0.5 min. Before the next injection, the column was re-equilibrated with 85% solvent A for 9.5 min (total sampling time of 35 min). Under these conditions, 2-quinoxalinol eluted between 6.2 and 6.6 min. Sodium dithionite present in activity assays affects the fluorescence of the 2-quinoxalinol derivative. Quantitative estimates for glyoxylate were thus obtained from a calibration curve of derivatized synthetic glyoxylate standards (3−100 μM) prepared and incubated as described for the activity assays lacking AdoMet, HydG, and tyrosine.

Data Analysis. Data were analyzed and graphs prepared using GraphPad Prism (version 6.00 for Windows, GraphPad Software, La Jolla, CA). At saturating substrate concentrations, the velocity data of all HydG variants were fit (R^2 > 0.98, except for WT $K_{M\ AdoMet}$, where R^2 = 0.93) to classical Michaelis−Menten kinetics[49,50] (eq 1).

$$\frac{v}{[\mathrm{HydG}]} = \frac{k_{cat}[S]}{K_M + [S]} \quad (1)$$

where v is the initial velocity, k_{cat} is the turnover number, [S] is the substrate concentration, and K_M is the Michaelis−Menten constant. Time courses were fit (R^2 > 0.97) to a first-order kinetic process (eq 2).

$$[P] = [P]_{max}(1 - e^{-kt}) \quad (2)$$

where [P] is the observed product concentration, $[P]_{max}$ is the maximal amount of product formed, and k is the observed first-order rate constant, or fit to linear product formation. The slope of this curve at time zero gives the initial rate of product formation ($v = [P]_{max}k$). Dividing the initial rate by the concentration of HydG gives the apparent turnover number, k_{cat}^{app}, as shown in eq 3.

$$k_{cat}^{app} = \frac{k[P]_{max}}{[\mathrm{HydG}]} \quad (3)$$

dx.doi.org/10.1021/bi401143s | *Biochemistry* 2013, 52, 8696−8707

RESULTS

HydG Contains Two [4Fe-4S] Clusters. *C. acetobutylicum* HydG was anaerobically purified by Ni-affinity chromatography and contained substoichiometric amounts of iron. After chemical reconstitution with 10 molar equiv of iron and sulfide in the presence of DTT, WT HydG contained on average 7.1 ± 1.1 irons per protein and showed a broad UV−visible absorption band around 410 nm (Figure 1), characteristic of

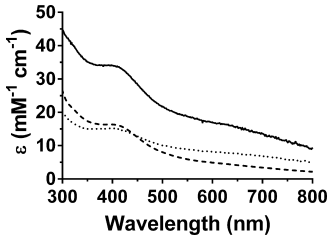

Figure 1. UV−visible characterization of HydG variants. Representative UV−visible spectra of WT [(—) 8.0 ± 0.9 Fe atoms/protein], C96/100/103A [(---) 3.4 ± 0.1 Fe atoms/protein], and ΔCTD HydG [(···) 3.6 ± 0.2 Fe atoms/protein].

$[4Fe\text{-}4S]^{2+}$ clusters.[51] On the basis of the protein concentration determined using the Bradford assay, the extinction coefficient at 400 nm was calculated to be 34 mM^{-1} cm^{-1}, in agreement with the presence of two $[4Fe\text{-}4S]^{2+}$ clusters[17,20] assuming an ε_{400} of 16 mM^{-1} cm^{-1}.[51] To characterize the individual clusters bound to the N- and C-terminal cysteine motifs of HydG, we prepared an N-terminal C96/100/103A triple mutant that cannot coordinate the radical AdoMet cluster and a ΔCTD mutant that is lacking the $CX_2CX_{22}C$ motif proposed to coordinate cluster II and amino acids thereafter. Both mutants were expressed as soluble and stable proteins, suggesting that neither cluster is required for the folding of the protein in a soluble form. Iron analyses after *in vitro* reconstitution with 5−6 molar equiv of iron and sulfide indicated the presence of 3.4 ± 0.1 irons per C96/100/103A HydG and 3.1 ± 0.4 irons per ΔCTD HydG (Table S1 of the Supporting Information). The corresponding UV−visible spectra are characteristic of a $[4Fe\text{-}4S]^{2+}$ cluster (Figure 1), and the calculated molar extinction coefficients (ε_{400}) of approximately 16 mM^{-1} cm^{-1} suggest the presence of a single $[4Fe\text{-}4S]^{2+}$ cluster in C96/100/103A and ΔCTD HydG, in agreement with the iron analyses.

EPR spectroscopy was used to confirm the presence of $[4Fe\text{-}4S]$ clusters and to allow a more detailed characterization. Photoreduced, reconstituted WT HydG has previously been characterized and displayed g values of 2.03, 1.92, and 1.90 in the absence of AdoMet, while two distinct rhombic signals were observed (g_1 values of 2.02, 1.93, and 1.91; g_2 values of 2.00, 1.87, and 1.83) in the presence of AdoMet.[17] For ease of comparison, these spectra are reproduced in Figure 2A. The observation of 0.48 spin/protein in photoreduced WT HydG samples in the absence and 0.88 spin/protein in the presence of AdoMet suggests that binding of AdoMet to cluster I increases its redox potential. This is in accord with spectroelectrochemical results that showed that the redox potential of the $[4Fe\text{-}4S]^{2+/+}$ couple in the radical AdoMet enzyme lysine-2,3-

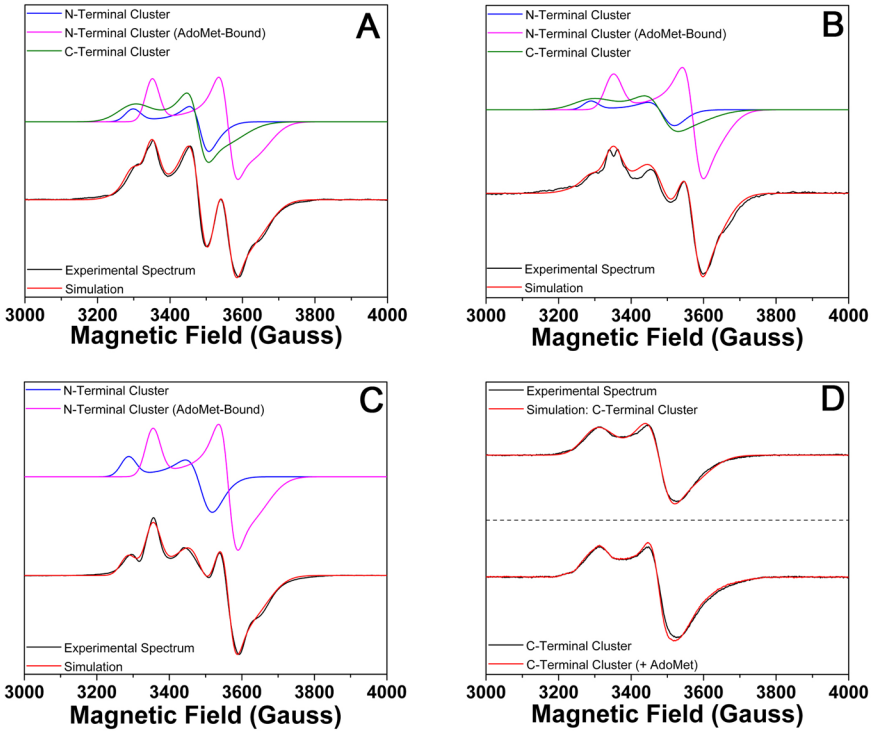

Figure 2. X-Band EPR spectra of reduced, reconstituted HydG variants in the presence of 1 mM AdoMet (12 K). (A) Photoreduced WT HydG (65 μM, 8.7 ± 0.7 Fe atoms/protein). (B) Dithionite-reduced WT HydG (101 μM, 6.5 ± 0.1 Fe atoms/protein). (C) Photoreduced ΔCTD HydG (424 μM, 2.4 ± 0.2 Fe atoms/protein). Experimental spectra are colored black, while composite simulations are colored red. Spectral components to the simulated signal are depicted in the top part of each panel. (D) The bottom part of the panel shows the spectrum for photoreduced C96/100/103A HydG (90 μM, 3.4 ± 0.1 Fe atoms/protein) in the absence (black) and presence of 1 mM AdoMet (red), and the top part of the panel shows the experimental spectrum of the photoreduced enzyme (black) and the corresponding simulation spectrum (red). Samples were prepared in 50 mM Hepes, 0.5 M KCl, and 5% (w/v) glycerol (pH 7.4). See Materials and Methods for EPR spectrometer parameters.

dx.doi.org/10.1021/bi401143s | *Biochemistry* 2013, 52, 8696−8707

aminomutase is increased from −480 to −430 mV in the presence of AdoMet.[52] It should be noted that some batch to batch variability was observed in the extent of additional cluster I reduction for the WT enzyme when AdoMet was present (data not shown). Addition of the AdoMet analogue *S*-adenosyl-L-homocysteine (AdoHcy, 1 mM) to WT HydG had no observable effect on the reduced WT HydG spectrum (data not shown). While there is little difference between photoreduced and dithionite-reduced HydG spectra with regard to the overall line shape and *g* values, the fraction of reduced AdoMet-bound cluster I was found to be slightly higher in dithionite-reduced than in photoreduced HydG samples as exemplified for WT HydG in panels A and B of Figure 2 and panels A and B of Figure S1 of the Supporting Information (see also Table S2 of the Supporting Information).

The $S = {}^1/_2$ signal in the EPR spectrum of photoreduced, reconstituted ΔCTD HydG closely resembles the WT resonance, with *g* values of 2.03, 1.92, and 1.90 (Figure S1C of the Supporting Information). As seen for WT HydG, addition of AdoMet generates a rhombic signal (*g* values of 2.00, 1.88, and 1.84) and a mostly axial signal (*g* values of 2.04, 1.92, and 1.90) representing AdoMet-bound and unbound cluster I, respectively (Figure 2C). Simulation of the data suggests that 73% of the overall signal arises from AdoMet-bound cluster I. Spin quantification in the absence (0.31 spin/protein) and presence of AdoMet (0.39 spin/protein) indicates that the radical AdoMet [4Fe-4S] cluster is only partially reduced in either case.

Photoreduced, reconstituted C96/100/103A HydG displayed a broad signal with *g* values of 2.03, 1.92, and 1.88 (Figure 2D, bottom panel, black trace). This spectrum is similar to that of reduced WT HydG and unambiguously demonstrates that the C-terminal cysteine residues can also coordinate a [4Fe-4S] cluster. The observed values of 0.41 spin/protein in the absence and 0.43 spin/protein in the presence of AdoMet are very close to those of the $[4Fe\text{-}4S]^+$ clusters quantified for ΔCTD HydG and suggest similar redox potentials for clusters I and II. Although the similarity of these EPR resonances points toward comparable electronic environments of each cluster, addition of AdoMet to the C96/100/103A mutant in >10-fold excess did not cause a significant signal perturbation (Figure 2D, bottom panel, red trace), suggesting that cluster II cannot substitute for cluster I with regard to AdoMet binding.

EPR analyses of the HydG variants lacking the N- or C-terminal cluster allowed extraction of the signals deriving from the individual clusters. Spectral summation of these N- and C-terminal cluster signals in a near 1:1 ratio accurately simulates the reduced WT HydG spectrum (Figure S1A,B and Table S2 of the Supporting Information), suggesting that both clusters behave independently, with no observable coupling in the absence of AdoMet. The observation that AdoMet does not interact with cluster II allowed for detailed simulation of the reduced WT spectrum in the presence of AdoMet by additionally including the AdoMet-bound cluster I signal.

The C-terminal cysteine motif contains only three conserved cysteine residues, indicating that cluster II is site differentiated, with one iron available for potential tyrosine coordination in a mode similar to that of binding of AdoMet to cluster I. Coordination of the substrate to the auxiliary [4Fe-4S] cluster was experimentally observed for MoaA[53,54] and was implicated for TYW1.[55] The presence of 1 mM tyrosine or AdoHcy and tyrosine (1 mM each) caused subtle perturbations of the EPR spectrum of the dithionite-reduced WT enzyme (Figure S2 of the Supporting Information), which may be indicative of coordination of tyrosine to cluster II. In the absence of additional experimental evidence, however, it is difficult to verify this. The absence of signal perturbation in the dithionite-reduced WT HydG spectrum upon addition of AdoHcy suggests that it does not substitute for AdoMet. In a separate experiment, we explored the possibility that the binding of tyrosine to cluster II occurs only in the presence of AdoMet by using the C96/100/103A variant protein (data not shown). These EPR spectra revealed similar slight perturbations to the paramagnetic signatures associated with the reduced cluster II signals as shown in Figure S2 of the Supporting Information, indicating that either tyrosine does not coordinate cluster II or its coordination does not substantially perturb cluster *g* values.

These results collectively support a role for the C-terminal cluster and/or amino acid residues in the C-terminus in contributing to the proper orientation of substrates in the active site, as well as ensuring efficient N-terminal cluster reduction.

Characterization of the C386S HydG Single Mutant. A C386S HydG single mutant was reconstituted with 10 molar equiv rather than 5 molar equiv of iron and sulfide to investigate whether the single amino acid change and the similarity of the ability of serine and cysteine to act as cluster ligands[56−58] are sufficient for partial or full assembly of cluster II. Reconstituted C386S HydG contained on average 4.9 ± 1.1 irons per protein and showed a slightly decreased absorbance at 410 nm compared to that of reconstituted WT HydG (Figure S3 of the Supporting Information). This suggests that cluster II might be present in only a fraction of C386S HydG or, alternatively, may only be partially assembled, for example, as a [3Fe-4S] cluster.[59] The UV−visible spectrum supports the absence of [2Fe-2S] clusters that have strong characteristic absorption maxima at 330, 420, and 460 nm.[60] Parallel EPR studies of dithionite-reduced C386S HydG (Figure S4A of the Supporting Information) also excluded [2Fe-2S] clusters as the $S = {}^1/_2$ signal can be observed only below 30 K (data not shown). This EPR resonance is more rhombic than that of WT HydG and was best simulated as 86% reduced cluster I (*g* values of 2.03, 1.93, and 1.89) and 14% reduced cluster II (*g* values of 2.02, 1.93, and 1.86). Addition of AdoMet gave rise to a clear rhombic signal (*g* values of 2.00, 1.89, and 1.84) for AdoMet-bound cluster I, with an approximately 10% contribution from the reduced C-terminal cluster (*g* values of 2.04, 1.93, and 1.87) (Figure S4B of the Supporting Information). The small amount of reduced cluster II required to simulate the spectrum is in accord with the decreased amount of iron quantified compared to that for WT HydG.

Determination of Substrate Michaelis−Menten Constants for WT and Mutant HydG. We set out to determine the Michaelis−Menten constants for AdoMet and tyrosine ($K_{M\ AdoMet}$ and $K_{M\ TYR}$, respectively) (i) to investigate whether any observed reduction in the level of formation of cyanide by HydG mutants[39,40] was due to a decrease in the rate of tyrosine cleavage or a decreased affinity of the AdoMet and/or tyrosine substrates for these enzymes and (ii) to use this information to optimize activity assays for more accurate detection of AdoMet- and tyrosine-derived cleavage products. Unsurprisingly, the N-terminal C96/100/103A triple mutant (100 μM) was unable to cleave AdoMet to 5′-dAH upon being incubated with 1 mM AdoMet, 1 mM tyrosine, and 5 mM sodium dithionite at 37 °C for 60 min because of the lack of AdoMet binding cluster I. Accordingly, this mutant was not included in the following study.

dx.doi.org/10.1021/bi401143s | *Biochemistry* 2013, 52, 8696−8707

To assess tyrosine cleavage, initial rates of *p*-cresol formation were determined. The slow reaction catalysis by HydG ($k_{cat} < 2 \times 10^{-3}$ s^{-1})[16] limited the number of turnovers that could be measured. As a result, the initial rates may not have been determined under ideal steady state conditions. Another consequence of slow turnover was the requirement, at low substrate concentrations, to add relatively high concentrations of HydG (5 μM) to achieve measurable turnover. This gave equimolar concentrations of the enzyme and substrate for the lowest AdoMet and tyrosine concentrations, conditions at which the free ligand assumption ($[S]_{total} \cong [S]_{free}$ for Michaelis–Menten kinetics) is not valid. For these two reasons, the associated Michaelis–Menten constants should be treated as approximate values.

At saturating tyrosine concentrations (400 μM for WT and 3 mM for mutant HydG), the velocity data of all HydG variants were best fit to classical Michaelis–Menten kinetics[49,50] (eq 1 and Figure 3A). The $K_{M\ AdoMet}$ values for WT (2.6 ± 1.1 μM) and ΔCTD HydG (3.6 ± 0.7 μM) are identical within error, whereas the $K_{M\ AdoMet}$ for C386S HydG was calculated to be 17.4 ± 2.6 μM (Table 1). At higher AdoMet concentrations (>300 μM), an activity decrease for WT but not for mutant HydG was observed, which may be due to a decreased assay pH caused by the presence of residual trifluoroacetic acid in the employed AdoMet samples.

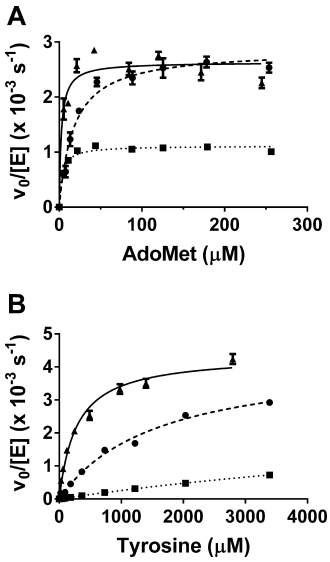

Figure 3. Substrate-dependent initial rates of *p*-cresol formation by HydG variants. Initial rates (v_0/[E]) of formation of *p*-cresol by HydG (5 μM) in 50 mM Hepes, 0.5 M KCl buffer (pH 7.4) at 37 °C. Assays additionally contained 1 mM sodium dithionite and (A) tyrosine (400 μM for WT and 3 mM for mutants) and varying AdoMet concentrations or (B) AdoMet (100 μM for WT and 200 μM for mutants) and varying tyrosine concentrations. The data were fit to Michaelis–Menten kinetics (eq 1). Calculated kinetic parameters for WT (—▲—), C386S (---●---), and ΔCTD HydG (···■···) are summarized in Table 1.

At saturating AdoMet concentrations (100 μM for WT and 200 μM for mutants), the *p*-cresol velocity data were also fit to eq 1 (Figure 3B) and the $K_{M\ TYR}$ for WT HydG was calculated to be 278.9 ± 34.0 μM (Table 1). This K_M value is 1 order of magnitude higher than most reported substrate K_M values of other radical AdoMet enzymes,[61−63] but it lies below the intracellular tyrosine concentration of *C. acetobutylicum* ATCC824 during acidogenesis (640 μM) and solventogenesis (660 μM),[64] ensuring that HydG would be able to respond to fluctuations in tyrosine concentration during both stages of cell growth. Bearing in mind the assumptions required when treating a K_M as an apparent binding constant,[65] we found the increased $K_{M\ TYR}$ constants for C386S and ΔCTD HydG of 1.6 ± 0.2 and 10.6 ± 0.6 mM, respectively, clearly show that modifications to the C-terminal cluster decrease the apparent affinity for tyrosine. The similarity of the turnover number (k_{cat}) values for *p*-cresol formation between ΔCTD HydG (3.0 × 10^{-3} s^{-1}) and WT and C386S values (4.3 × 10^{-3} s^{-1}) (Table 1) is consistent with a model in which the rate of radical formation and tyrosine cleavage is unaffected in the variant proteins. This suggests that catalytic steps can be rescued at higher tyrosine concentrations. Experimentally, this is observed for C386S HydG, but it is experimentally difficult to fully saturate ΔCTD HydG because of the limited solubility of tyrosine in assay buffer at physiological pH.[66]

Table 1. AdoMet- and Tyrosine-Dependent Kinetic Parameters for WT and Mutant HydG (Figure 3)[a]

HydG	$K_{M\ AdoMet}$ (μM)	$k_{cat\ AdoMet}$ (×10^{-3} s^{-1})	$K_{M\ TYR}$ (mM)	$k_{cat\ TYR}$ (×10^{-3} s^{-1})
WT	2.6 ± 1.1	2.6 ± 0.1	0.3 ± 0.0 (3)	4.4 ± 0.2
C386S	17.4 ± 2.6	2.9 ± 0.1	1.6 ± 0.2[b]	4.3 ± 0.3[b]
ΔCTD	3.6 ± 0.7	1.1 ± 0.0 (3)	10.6 ± 0.6[b]	3.0 ± 0.1[b]

[a]Initial rates of AdoMet- and tyrosine-dependent *p*-cresol formation were fit to Michaelis–Menten kinetics (eq 1). [b]These values should be regarded as approximate. For the ΔCTD HydG, the apparent K_M is above the highest concentration investigated, and for the C386S mutant, only two data points were obtained above K_M. The solubility of tyrosine limited the measurements that were possible at higher tyrosine concentrations.

Kinetic Characterization of WT and Mutant HydG. We previously observed catalytic formation of *p*-cresol and cyanide in a 1:1 ratio by WT HydG in the presence of AdoMet, tyrosine, and sodium dithionite (1 mM each).[16] Taking advantage of the determined Michaelis–Menten constants for AdoMet and tyrosine (Table 1), we repeated these time course experiments under optimized assay conditions (40 μM HydG, 0.5 mM AdoMet, 4 mM tyrosine, and 1 mM sodium dithionite) to compare formation of the tyrosine cleavage products cyanide and glyoxylate as well as the AdoMet cleavage product 5′-dAH relative to the formation of *p*-cresol. Under these conditions, all HydG proteins use AdoMet as a substrate, as reflected in the formation of 5′-dAH, and cleave tyrosine catalytically (Figure 4). The employed concentration of AdoMet represents a compromise between the observed inhibition of WT HydG (significant above 300 μM AdoMet) and the problem of AdoMet becoming limiting upon multiple turnovers (increasingly a problem at low AdoMet concentrations). In fact, the inhibition of WT HydG remained a significant problem as we observed a 50% decrease in the level of *p*-cresol formation by WT HydG [k_{cat}^{app} = (1.8 ± 0.2) × 10^{-3} s^{-1}] compared to that of C386S HydG [k_{cat}^{app} = (4.6 ± 0.2) × 10^{-3} s^{-1}] (Figure 4A,B and Table 2). Over a 60 min time period, ΔCTD HydG formed quantities of *p*-cresol similar to that formed by the (inhibited) WT enzyme with a k_{cat}^{app} of (1.1 ± 0.1) × 10^{-3} s^{-1} (Figure 4C and Table 2). This observed apparent k_{cat} compares very well with the rate for the previously observed tyrosine-dependent *p*-cresol formation (Figure 3B), and bearing in mind that ΔCTD HydG cannot be experimentally saturated with tyrosine, we suggest that neither the auxiliary cluster II nor the C-terminal

dx.doi.org/10.1021/bi401143s | *Biochemistry* 2013, 52, 8696−8707

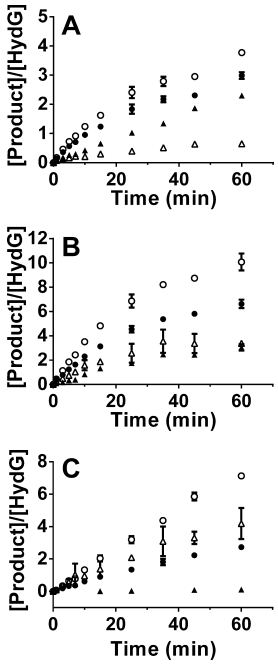

Figure 4. Time-dependent HydG-catalyzed AdoMet and tyrosine cleavage. Formation of molar equivalents of 5′-dAH (○), *p*-cresol (●), cyanide (▲), and glyoxylate (△) with respect to (A) WT (40 μM, 8.0 ± 0.9 Fe atoms/protein), (B) C386S (40 μM, 6.4 ± 0.8 Fe atoms/protein), and (C) ΔCTD HydG (40 μM, 3.6 ± 0.2 Fe atoms/protein) in the presence of AdoMet (0.5 mM), tyrosine (4 mM), and sodium dithionite (1 mM) in 50 mM Hepes, 0.5 M KCl assay buffer (pH 7.4). The data represent the average of duplicate assays conducted at 37 °C and are shown with standard deviations. The data were modeled (not shown for the sake of clarity) with first-order kinetics (eq 2) to yield the respective turnover numbers summarized in Table 2.

Table 2. Apparent Turnover Numbers for HydG-Catalyzed AdoMet and Tyrosine Cleavage (Figure 4)[a]

	k_{cat}^{app} ($\times 10^{-3}$ s^{-1})		
product	WT	C386S	ΔCTD
5′-dAH	2.3 ± 0.3	6.9 ± 0.3	2.3 ± 1.1
p-cresol	1.8 ± 0.2	4.6 ± 0.2	1.1 ± 0.1
cyanide	0.6 ± 0.0 (2)[b]	1.6 ± 0.4	NA[c]
glyoxylate	0.5 ± 0.1	4.2 ± 0.9	1.5 ± 0.3

[a]Data were fit to first-order kinetics (eq 2), and the apparent turnover number was extracted using eq 3. [b]A fit to eq 2 was not successful, and cyanide formation was modeled with linear kinetics. [c]Not applicable.

residues (after C386) are essential for the cleavage of tyrosine from *p*-cresol.

The nonaromatic product of ThiH-catalyzed tyrosine C_α–C_β bond cleavage is hypothesized to be dehydroglycine.[32] Dehydroglycine is hydrolytically unstable and yields glyoxylate *in vitro*. While stoichiometric quantities of glyoxylate with respect to *p*-cresol were identified in ThiH activity assays, little glyoxylate accumulated during HydG turnover. Instead, a 1:1 ratio of cyanide to *p*-cresol was observed,[16] suggesting that dehydroglycine (or the closely related glycine C_α-centered radical) is an intermediate during cyanide synthesis (Scheme 1, step B). In this study, we observed some variation in the cyanide stoichiometry compared to that with *p*-cresol for different WT HydG samples. At the 60 min time point for batch A, a *p*-cresol:cyanide ratio of 2.5:1 was observed, whereas for batch B, the ratio was 1.3:1 (Figure 4A). The reduced level of cyanide formation compared to that of *p*-cresol was completely ascribed to detection of increased amounts of glyoxylate. We hypothesize that glyoxylate accumulates *in vitro* if the reaction step from dehydroglycine (or a closely related intermediate) to cyanide and CO formation (Scheme 1, step B) is very slow or indeed aborted. The varying amounts of cyanide formed indicate that some batch to batch variation can be observed in reconstituted HydG samples, although no significant differences in the iron quantification and UV–visible spectra were observed. This variation makes it difficult to accurately assess the role of the C-terminal cysteine motif and coordinated cluster II with respect to cyanide formation for the C386S HydG mutant. The turnover number for cyanide formation by C386S HydG was on average 65% lower than that of *p*-cresol (Table 2), which is equivalent to a *p*-cresol:cyanide ratio of 2.2:1 after 60 min (Figure 4B). Again, the remaining tyrosine cleavage product is accounted for by glyoxylate. It is interesting to note that while the WT enzyme formed 1.5–2.3 molar equiv of cyanide with respect to protein concentration, the C386S mutant catalyzed formation of 2.8 molar equiv of cyanide. Although ΔCTD HydG catalyzed formation of 100 μM *p*-cresol over a 60 min period (Figure 4C), representing a 60-fold improvement in activity compared to observations by Tron[40] for *Ca* or *Tte* ΔCTD HydG, the amounts of detected cyanide reported herein were very small (4.6 ± 0.6 μM, 0.12 mol/mol of ΔCTD). Instead, almost 100% glyoxylate with respect to *p*-cresol was formed. Importantly, none of the C-terminally modified HydG variants formed detectable amounts of CO.

DISCUSSION

In addition to the canonical radical AdoMet CX_3CX_2C motif found close to the N-terminus, *Ca* HydG contains a C-terminal $CX_2CX_{22}C$ cysteine triad, proposed to coordinate a second [4Fe-4S] cluster. While the C-terminal motif is not completely conserved among different organisms,[37] its requirement for HydG activity during [FeFe]-hydrogenase activation has been demonstrated by mutagenesis.[36] Using an N-terminal C96/100/103A mutant and a truncated ΔCTD HydG variant lacking the 87 C-terminal residues, we have used UV–visible and EPR spectroscopy together with iron analyses to independently characterize the [4Fe-4S] cluster in these variants, and the results unambiguously demonstrate that the C-terminal cysteine triad in WT HydG coordinates an auxiliary [4Fe-4S] cluster. The EPR spectra of reduced C96/100/103A and ΔCTD HydG both displayed remarkably similar *g* values compared to that of WT HydG, which suggests the N- and C-terminal clusters occupy similar electronic environments. Analysis of the EPR spectra does not, however, unequivocally identify the nature of the fourth ligand to the C-terminal cluster. While addition of AdoMet to reduced ΔCTD HydG samples gave a rhombic EPR signal, characteristic of an AdoMet-bound [4Fe-4S] cluster, a similar change in line shape was not observed for the triple N-terminal mutant. These results suggest that while the N- and C-terminal clusters are both site-differentiated, AdoMet binding occurs only at the N-terminal radical AdoMet cluster. This explains the observed inability of the C96/100/103A HydG mutant to cleave AdoMet.

Independent characterization of each [4Fe-4S] cluster by EPR using the N- and C-terminal HydG variants allowed for the successful reconstruction of the WT reduced signal in the absence (Figure S1A,B of the Supporting Information) and

dx.doi.org/10.1021/bi401143s | *Biochemistry* 2013, 52, 8696–8707

presence of AdoMet (Figure 2A,B). These results clearly show that the reduced WT signal is best simulated as a near 1:1 mixture of N- and C-terminal [4Fe-4S]$^{+}$ clusters, while the observed signal change following AdoMet addition can be simulated by additionally including the AdoMet-bound cluster I signal. These simulations define the *g* values associated with the individual [4Fe-4S] cluster states in WT HydG more clearly (Table S2 of the Supporting Information) than simulations we previously employed.[17] As a result, we identified that the nearly doubled spin quantification in the WT HydG·AdoMet sample compared to that of WT HydG mostly reflects an enhanced reduction of the radical AdoMet and not the C-terminal auxiliary [4Fe-4S] cluster (Table S2 of the Supporting Information). For WT, C386S, and ΔCTD HydG, the extent of cluster reduction in the presence of AdoMet varied between protein preparations, likely depending on efficiency of cluster reconstitution, and this variability restricts a detailed interpretation of the data.

We used enzymatically synthesized AdoMet to determine the $K_{M\ AdoMet}$ in the presence of saturating tyrosine concentrations for WT, C386S, and ΔCTD HydG to be between 3 and 17 μM. Given that AdoMet coordinates to cluster I and is additionally involved in well-characterized hydrogen bonding interactions to residues not expected to be affected by the C386S mutation and C-terminal deletion,[23−25,67,68] it is not surprising that the affinity for AdoMet is very similar for these HydG variants. It further suggests that the introduced mutations do not strongly affect the positioning of AdoMet binding residues, implying correct folding of the characteristic core triosephosphate isomerase (TIM) barrel observed among radical AdoMet enzymes.[69]

The C386S HydG mutant showed a 5-fold decrease in the apparent tyrosine affinity compared to that of WT HydG, suggesting a significant role for the auxiliary [4Fe-4S] cluster in the recognition and/or binding of tyrosine. On the basis of these results, it is intriguing that addition of tyrosine with AdoHcy introduced slight changes into the EPR spectrum of dithionite-reduced WT HydG, but additional experiments are required to verify the binding of tyrosine to cluster II. Deleting the HydG C-terminal domain decreases the apparent affinity for tyrosine an additional 7-fold compared to that of C386S HydG and could point toward additional binding interactions between tyrosine and amino acids in the C-terminal domain.

Using the determined substrate Michaelis−Menten constants, we conducted comparative *in vitro* activity assays. The WT, C386S, and ΔCTD HydG enzymes all cleaved tyrosine catalytically with apparent *p*-cresol k_{cat} values ranging between 1.1 and 4.6 × 10^{-3} s^{-1}. This agrees well with our previous WT HydG characterization[16] and product formation rates observed for other radical AdoMet enzymes.[70] Bearing in mind that the ΔCTD HydG enzyme cannot be saturated with tyrosine because of experimental limitations (the solubility of tyrosine), we find the observed similarity in the amounts of *p*-cresol formed compared to that for (partially inhibited) WT HydG indicates that tyrosine cleavage can continue in a manner predominantly independent of the C-terminal domain. With the observed affinity decrease for tyrosine after removal of the C-terminus (suggesting some interactions with these amino acid residues), it appears that spatially distinct and additive binding contacts to tyrosine can be established but that initiation of tyrosine cleavage occurs inside the TIM barrel. This is in accord with HydG and ThiH sharing similar patches of conserved amino acid residues positioned at the internal face of the β-sheets of the TIM barrel.[15]

Spectral EPR simulations furthermore allowed the deconvolution of the cluster components present in reduced C386S HydG to be approximated as 13% cluster II compared to 46% simulated for WT HydG. The observation that WT and C386S HydG catalyzed cyanide formation with the same relative rates compared to that of *p*-cresol implies that cluster II is not required for cyanide synthesis, as previously suggested by Nicolet and co-workers.[39] While substoichiometric detection of CO in WT HydG assays[17,39] indicated the formation of a strong iron−carbonyl complex, the formation of 2.8 molar equiv of cyanide by C386S HydG (after 60 min) argues against the coordination of cyanide to cluster II.

The levels of cyanide apparently formed by ΔCTD HydG are very low (4−5 μM); in fact, they are so close to our quantification limit (5 μM) that they may represent a "false positive". In any case, the formation of 100 μM *p*-cresol and glyoxylate but negligible cyanide by ΔCTD HydG supports the notion that C-terminal amino acid residues are required for cyanide synthesis.[39] In conclusion, our collective data support a model in which deletion of the *Ca* HydG C-terminal domain is at worst only mildly deleterious to the AdoMet and tyrosine cleavage steps but strongly affects the steps leading to cyanide and CO formation. In this regard, C-terminally truncated *Ca* HydG strongly resembles ThiH.[32]

The auxiliary [4Fe-4S] clusters of the radical AdoMet-dependent Cys- and Ser-type anaerobic sulfatase-modifying enzymes[71,72] and the 2-deoxy-*scyllo*-inosamine dehydrogenase BtrN[73,74] have been proposed to act as electron acceptors. This was evidenced in BtrN by an EPR silent mutant not containing the radical AdoMet cluster and the appearance of a new EPR signal during WT BtrN turnover, suggesting a very low redox potential for auxiliary cluster II in WT BtrN, which is however reduced during catalysis of the reaction. A similar electron transfer role could be envisaged for the *Ca* HydG C-terminal cluster to permit the interconversion between the tyrosine-derived dehydroglycine and the glycine radical (Scheme 1). EPR analyses of the C96/100/103A HydG mutant showed a broad signal, confirming that (in contrast to BtrN) cluster II in HydG can readily be reduced. In principle, tyrosine can be cleaved homolytically or heterolytically to form a C-centered glycine radical or dehydroglycine, respectively (Scheme 1, step A). While formation of the glycine radical is thermodynamically favored,[32] our *in vitro* observations that significant amounts of the dehydroglycine hydrolysis product glyoxylate are formed by the C386S and ΔCTD HydG mutants (which contain little or no C-terminal cluster) point toward heterolytic cleavage of tyrosine to form dehydroglycine. Because of the reducing assay conditions and the absence of cluster II, it is not evident how the postulated glycine radical could be oxidized to dehydroglycine. When considering the stoichiometry of reaction products, decarbonylation of the dehydroglycine intermediate can potentially yield cyanide and CO products.[16] We have confirmed the observation[39] that none of the C-terminal *Ca* HydG mutants formed CO. The apparent requirement for cluster II supports an alternative hypothesis that holds that the reduced cluster II may provide one electron for reversible reduction of dehydroglycine to the C-centered glycine radical (Scheme 1). In this hypothesis, deletion of the HydG C-terminal domain prevents formation of the glycine radical from dehydroglycine. The mechanism by which one of these

intermediates is converted to cyanide and CO will require further elucidation.[75]

■ ASSOCIATED CONTENT

Supporting Information

Summary of the iron content of reconstituted HydG variants, EPR spectra of HydG variants in the absence of AdoMet, UV−visible and EPR spectra of C386S HydG, and a summary of EPR (simulation) parameters. This material is available free of charge via the Internet at http://pubs.acs.org.

■ AUTHOR INFORMATION

Corresponding Author

*E-mail: p.l.roach@soton.ac.uk. Phone: (+44) 2380 5959 19.

Funding

This work was supported by the University of Southampton, U.S. Department of Energy Grant DE-FG02-10ER16194 (to J.B.B. and J.W.P.), and National Aeronautic and Space Administration Astrobiology Institute Grant NNA08CN85A (to J.W.P. and J.B.B.).

Notes

The authors declare no competing financial interest.

■ ACKNOWLEDGMENTS

We thank M. J. Hiscox (Chemistry, University of Southampton) and Richard Cammack (Pharmaceutical Science Research Division, King's College London, London, U.K.) for insightful discussions and Christie Green (Montana State University) for assistance in preparing ΔCTD HydG.

■ ABBREVIATIONS

AdoHcy, *S*-adenosyl-L-homocysteine; AdoMet, *S*-adenosyl-L-methionine; *Ca*, *C. acetobutylicum*; *CpI*, *C. pasteurianum*; 5′-dAH, 5′-deoxyadenosine; DTT, dithiothreitol; EPR, electron paramagnetic resonance; FAS, ferrous ammonium sulfate; FTIR, Fourier transform infrared; HPLC, high-pressure liquid chromatography; PMSF, phenylmethanesulfonyl fluoride; TIM, triosephosphate isomerase; *Tte*, *T. tengcongensis*; WT, wild type.

■ REFERENCES

(1) Vignais, P. M., and Billoud, B. (2007) Occurrence, Classification, and Biological Function of Hydrogenases: An Overview. *Chem. Rev. 107*, 4206−4272.

(2) Shima, S., and Thauer, R. K. (2007) A third type of hydrogenase catalyzing H_2 activation. *Chem. Rec. 7*, 37−46.

(3) Peters, J. W., Lanzilotta, W. N., Lemon, B. J., and Seefeldt, L. C. (1998) X-ray Crystal Structure of the Fe-Only Hydrogenase (*CpI*) from *Clostridium pasteurianum* to 1.8 Angstrom Resolution. *Science 282*, 1853−1858.

(4) Nicolet, Y., Piras, C., Legrand, P., Hatchikian, C. E., and Fontecilla-Camps, J. C. (1999) *Desulfovibrio desulfuricans* iron hydrogenase: The structure shows unusual coordination to an active site Fe binuclear center. *Structure 7*, 13−23.

(5) Nicolet, Y., de Lacey, A. L., Vernède, X., Fernandez, V. M., Hatchikian, E. C., and Fontecilla-Camps, J. C. (2001) Crystallographic and FTIR Spectroscopic Evidence of Changes in Fe Coordination Upon Reduction of the Active Site of the Fe-Only Hydrogenase from *Desulfovibrio desulfuricans*. *J. Am. Chem. Soc. 123*, 1596−1601.

(6) Ryde, U., Greco, C., and De Gioia, L. (2010) Quantum Refinement of [FeFe] Hydrogenase Indicates a Dithiomethylamine Ligand. *J. Am. Chem. Soc. 132*, 4512−4513.

(7) Silakov, A., Wenk, B., Reijerse, E., and Lubitz, W. (2009) ^{14}N HYSCORE investigation of the H-cluster of [FeFe] hydrogenase: Evidence for a nitrogen in the dithiol bridge. *Phys. Chem. Chem. Phys. 11*, 6592−6599.

(8) Mulder, D. W., Ortillo, D. O., Gardenghi, D. J., Naumov, A. V., Ruebusch, S. S., Szilagyi, R. K., Huynh, B., Broderick, J. B., and Peters, J. W. (2009) Activation of $HydA^{\Delta EFG}$ requires a preformed [4Fe-4S] cluster. *Biochemistry 48*, 64240−66248.

(9) Mulder, D. W., Boyd, E. S., Sarma, R., Lange, R. K., Endrizzi, J. A., Broderick, J. B., and Peters, J. W. (2010) Stepwise [FeFe]-hydrogenase H-cluster assembly revealed in the structure of $HydA^{\Delta EFG}$. *Nature 465*, 248−251.

(10) McGlynn, S. E., Shepard, E. M., Winslow, M. A., Naumov, A. V., Duschene, K. S., Posewitz, M. C., Broderick, W. E., Broderick, J. B., and Peters, J. W. (2008) HydF as scaffold protein in [FeFe] hydrogenase H-cluster biosynthesis. *FEBS Lett. 582*, 2183−2187.

(11) Czech, I., Silakov, A., Lubitz, W., and Happe, T. (2010) The [FeFe]-hydrogenase maturase HydF from *Clostridium acetobutylicum* contains a CO and CN^- ligated iron cofactor. *FEBS Lett. 584*, 638−642.

(12) Shepard, E. M., McGlynn, S. E., Bueling, A. L., Grady-Smith, C. S., George, S. J., Winslow, M. A., Cramer, S. P., Peters, J. W., and Broderick, J. B. (2010) Synthesis of the 2Fe subcluster of the [FeFe]-hydrogenase H cluster on the HydF scaffold. *Proc. Natl. Acad. Sci. U.S.A. 107*, 10448−10453.

(13) Mansure, J. J., and Hallenbeck, P. C. (2008) *Desulfovibrio vulgaris* Hildenborough HydE and HydG interact with the HydA subunit of the [FeFe] hydrogenase. *Biotechnol. Lett. 30*, 1765−1769.

(14) Kuchenreuther, J. M., Britt, R. D., and Swartz, J. R. (2012) New Insights into [FeFe] Hydrogenase Activation and Maturase Function. *PLoS One 7*, e45850.

(15) Pilet, E., Nicolet, Y., Mathevon, C., Douki, T., Fontecilla-Camps, J. C., and Fontecave, M. (2009) The role of the maturase HydG in [FeFe]-hydrogenase active site synthesis and assembly. *FEBS Lett. 583*, 506−511.

(16) Driesener, R. C., Challand, M. R., McGlynn, S. E., Shepard, E. M., Boyd, E. S., Broderick, J. B., Peters, J. W., and Roach, P. L. (2010) [FeFe]-Hydrogenase Cyanide Ligands Derived from *S*-Adenosylmethionine-Dependent Cleavage of Tyrosine. *Angew. Chem., Int. Ed. 49*, 1687−1690.

(17) Shepard, E. M., Duffus, B. R., George, S. J., McGlynn, S. E., Challand, M. R., Swanson, K. D., Roach, P. L., Cramer, S. P., Peters, J. W., and Broderick, J. B. (2010) [FeFe]-Hydrogenase Maturation: HydG-Catalyzed Synthesis of Carbon Monoxide. *J. Am. Chem. Soc. 132*, 9247−9249.

(18) Kuchenreuther, J. M., George, S. J., Grady-Smith, C. S., Cramer, S. P., and Swartz, J. R. (2011) Cell-free H-cluster Synthesis and [FeFe] Hydrogenase Activation: All Five CO and CN^- Ligands Derive from Tyrosine. *PLoS One 6*, e20346.

(19) Nicolet, Y., Rubach, J. K., Posewitz, M. C., Amara, P., Mathevon, C., Atta, M., Fontecave, M., and Fontecilla-Camps, J. C. (2008) X-ray Structure of the [FeFe]-Hydrogenase Maturase HydE from *Thermotoga maritima*. *J. Biol. Chem. 283*, 18861−18872.

(20) Rubach, J. K., Brazzolotto, X., Gaillard, J., and Fontecave, M. (2005) Biochemical characterization of the HydE and HydG iron-only hydrogenase maturation enzymes from *Thermatoga maritima*. *FEBS Lett. 579*, 5055−5060.

(21) Sofia, H. J., Chen, G., Hetzler, B. G., Reyes-Spindola, J. F., and Miller, N. E. (2001) Radical SAM, a novel protein superfamily linking unresolved steps in familiar biosynthetic pathways with radical mechanisms: Functional characterization using new analysis and information visualization methods. *Nucleic Acids Res. 29*, 1097−1106.

(22) Frey, P. A., Hegeman, A. D., and Ruzicka, F. J. (2008) The radical SAM superfamily. *Crit. Rev. Biochem. Mol. Biol. 43*, 63−88.

(23) Walsby, C., Ortillo, D., Broderick, W. E., Broderick, J. B., and Hoffman, B. M. (2002) An Anchoring Role for FeS Clusters: Chelation of the Amino Acid Moiety of *S*-Adenosylmethionine to the Unique Iron Site of the [4Fe-4S] Cluster of Pyruvate Formate-Lyase Activating Enzyme. *J. Am. Chem. Soc. 124*, 11270−11271.

(24) Vey, J. L., and Drennan, C. L. (2011) Structural Insights into Radical Generation by the Radical SAM Superfamily. *Chem. Rev. 111*, 2487−2506.
(25) Krebs, C., Broderick, W. E., Henshaw, T. F., Broderick, J. B., and Huynh, B. H. (2002) Coordination of Adenosylmethionine to a Unique Iron Site of the [4Fe-4S] of Pyruvate Formate-Lyase Activating Enzyme: A Mössbauer Spectroscopic Study. *J. Am. Chem. Soc. 124*, 912−913.
(26) Walsby, C. J., Hong, W., Broderick, W. E., Cheek, J., Ortillo, D., Broderick, J. B., and Hoffman, B. M. (2002) Electron-Nuclear Double Resonance Spectroscopic Evidence That *S*-Adenosylmethionine Binds in Contact with the Catalytically Active $[4Fe\text{-}4S]^{+}$ Cluster of Pyruvate Formate-Lyase Activating Enzyme. *J. Am. Chem. Soc. 124*, 3143−3151.
(27) Nicolet, Y., Amara, P., Mouesca, J.-M., and Fontecilla-Camps, J. C. (2009) Unexpected electron transfer mechanism upon AdoMet cleavage in radical SAM proteins. *Proc. Natl. Acad. Sci. U.S.A. 106*, 14867−14871.
(28) Henshaw, T. F., Cheek, J., and Broderick, J. B. (2000) The $[4Fe\text{-}4S]^{1+}$ Cluster of Pyruvate Formate-Lyase Activating Enzyme Generates the Glycyl Radical on Pyruvate Formate-Lyase: EPR-Detected Single Turnover. *J. Am. Chem. Soc. 122*, 8331−8332.
(29) Magnusson, O. T., Reed, G. H., and Frey, P. A. (1999) Spectroscopic Evidence for the Participation of an Allylic Analogue of the 5′-Deoxyadenosyl Radical in the Reaction of Lysine 2,3-Aminomutase. *J. Am. Chem. Soc. 121*, 9764−9765.
(30) Decamps, L., Philmus, B., Benjdia, A., White, R., Begley, T. P., and Berteau, O. (2012) Biosynthesis of F_0, Precursor of the F_{420} Cofactor, Requires a Unique Two Radical-SAM Domain Enzyme and Tyrosine as Substrate. *J. Am. Chem. Soc. 134*, 18173−18176.
(31) Kriek, M., Martins, F., Leonardi, R., Fairhurst, S. A., Lowe, D. J., and Roach, P. L. (2007) Thiazole Synthase from *Escherichia coli*. *J. Biol. Chem. 282*, 17413−17423.
(32) Kriek, M., Martins, F., Challand, M. R., Croft, A., and Roach, P. L. (2007) Thiamine Biosynthesis in *Escherichia coli*: Identification of the Intermediate and By-Product Derived from Tyrosine. *Angew. Chem., Int. Ed. 46*, 9223−9226.
(33) Challand, M. R., Martins, F. T., and Roach, P. L. (2010) Catalytic Activity of the Anaerobic Tyrosine Lyase Required for Thiamine Biosynthesis in *Escherichia coli*. *J. Biol. Chem. 285*, 5240−5248.
(34) Zhang, Q., Li, Y., Chen, D., Yu, Y., Duan, L., Shen, B., and Liu, W. (2011) Radical-mediated enzymatic carbon chain fragmentation-recombination. *Nat. Chem. Biol. 7*, 154−160.
(35) Yu, Y., Duan, L., Zhang, Q., Liao, R., Ding, Y., Pan, H., Wendt-Pienkowski, E., Tang, G., Shen, B., and Liu, W. (2009) Nosiheptide Biosynthesis Featuring a Unique Indole Side Ring Formation on the Characteristic Thiopeptide Framework. *ACS Chem. Biol. 4*, 855−864.
(36) King, P. W., Posewitz, M. C., Ghirardi, M. L., and Seibert, M. (2006) Functional Studies of [FeFe] Hydrogenase Maturation in an *Escherichia coli* Biosynthetic System. *J. Bacteriol. 188*, 2163−2172.
(37) Duffus, B. R., Hamilton, T. L., Shepard, E. M., Boyd, E. S., Peters, J. W., and Broderick, J. B. (2012) Radical AdoMet enzymes in complex metal cluster biosynthesis. *Biochim. Biophys. Acta 1824*, 1254−1263.
(38) Lanz, N. D., and Booker, S. J. (2012) Identification and function of auxiliary iron−sulfur clusters in radical SAM enzymes. *Biochim. Biophys. Acta 1824*, 1196−1212.
(39) Nicolet, Y., Martin, L., Tron, C., and Fontecilla-Camps, J. C. (2010) A glycyl free radical as the precursor in the synthesis of carbon monoxide and cyanide by the [FeFe]-hydrogenase maturase HydG. *FEBS Lett. 584*, 4197−4202.
(40) Tron, C., Cherrier, M. V., Amara, P., Martin, L., Fauth, F., Fraga, E., Correard, M., Fontecave, M., Nicolet, Y., and Fontecilla-Camps, J. C. (2011) Further Characterization of the [FeFe]-Hydrogenase Maturase HydG. *Eur. J. Inorg. Chem. 2011*, 1121−1127.
(41) Challand, M. R., Salvadori, E., Driesener, R. C., Kay, C. W. M., Roach, P. L., and Spencer, J. (2013) Cysteine Methylation Controls Radical Generation in the Cfr Radical AdoMet rRNA Methyltransferase. *PLoS One 8*, e67979.
(42) Farrar, C. E., Siu, K. K. W., Howell, P. L., and Jarrett, J. T. (2010) Biotin Synthase Exhibits Burst Kinetics and Multiple Turnovers in the Absence of Inhibition by Products and Product-Related Biomolecules. *Biochemistry 49*, 9985−9996.
(43) Schluckebier, G., Kozak, M., Bleimling, N., Weinhold, E., and Saenger, W. (1997) Differential binding of *S*-adenosylmethionine, *S*-adenosylhomocysteine and Sinefungin to the adenine-specific DNA methyltransferase M.TaqI. *J. Mol. Biol. 265*, 56−67.
(44) Shapiro, S. K., and Ehninger, D. J. (1966) Methods for the analysis and preparation of adenosylmethionine and adenosylhomocysteine. *Anal. Biochem. 15*, 323−333.
(45) Bradford, M. M. (1976) A rapid and sensitive method for the quantitation of microgram quantities of protein utilizing the principle of protein-dye binding. *Anal. Biochem. 72*, 248−254.
(46) Fish, W. W. (1988) Rapid colorimetric micromethod for the quantitation of complexed iron in biological samples. *Methods Enzymol. 158*, 357−364.
(47) Stoll, S., and Schweiger, A. (2006) EasySpin, a comprehensive software package for spectral simulation and analysis in EPR. *J. Magn. Reson. 178*, 42−55.
(48) Pierik, A. J., Roseboom, W., Happe, R. P., Bagley, K. A., and Albracht, S. P. J. (1999) Carbon Monoxide and Cyanide as Intrinsic Ligands to Iron in the Active Site of [NiFe]-Hydrogenases. *J. Biol. Chem. 274*, 3331−3337.
(49) Michaelis, L., and Menten, M. (1913) Die Kinetik der Invertinwirkung. *Biochemistry Zeitung 49*, 333−369.
(50) Johnson, K. A., and Goody, R. S. (2011) The Original Michaelis Constant: Translation of the 1913 Michaelis−Menten Paper. *Biochemistry 50*, 8264−8269.
(51) Sweeney, W. V., and Rabinowitz, J. C. (1980) Proteins Containing 4Fe-4S Clusters: An Overview. *Annu. Rev. Biochem. 49*, 139−161.
(52) Hinckley, G. T., and Frey, P. A. (2006) Cofactor Dependence of Reduction Potentials for $[4Fe\text{-}4S]^{2+/1+}$ in Lysine 2,3-Aminomutase. *Biochemistry 45*, 3219−3225.
(53) Hänzelmann, P., and Schindelin, H. (2006) Binding of 5′-GTP to the C-terminal FeS cluster of the radical *S*-adenosylmethionine enzyme MoaA provides insights into its mechanism. *Proc. Natl. Acad. Sci. U.S.A. 103*, 6829−6834.
(54) Lees, N. S., Hänzelmann, P., Hernandez, H. L., Subramanian, S., Schindelin, H., Johnson, M. K., and Hoffman, B. M. (2009) ENDOR Spectroscopy Shows That Guanine N1 Binds to [4Fe-4S] Cluster II of the *S*-Adenosylmethionine-Dependent Enzyme MoaA: Mechanistic Implications. *J. Am. Chem. Soc. 131*, 9184−9185.
(55) Perche-Letuvée, P., Kathirvelu, V., Berggren, G., Clemancey, M., Latour, J.-M., Maurel, V., Douki, T., Armengaud, J., Mulliez, E., Fontecave, M., Garcia-Serres, R., Gambarelli, S., and Atta, M. (2012) 4-Demethylwyosine Synthase from *Pyrococcus abyssi* Is a Radical-*S*-adenosyl-l-methionine Enzyme with an Additional $[4Fe\text{-}4S]^{+2}$ Cluster That Interacts with the Pyruvate Co-substrate. *J. Biol. Chem. 287*, 41174−41185.
(56) Brereton, P. S., Duderstadt, R. E., Staples, C. R., Johnson, M. K., and Adams, M. W. W. (1999) Effect of Serinate Ligation at Each of the Iron Sites of the $[Fe_4S_4]$ Cluster of *Pyrococcus furiosus* Ferredoxin on the Redox, Spectroscopic, and Biological Properties. *Biochemistry 38*, 10594−10605.
(57) Mansy, S. S., Xiong, Y., Hemann, C., Hille, R., Sundaralingam, M., and Cowan, J. A. (2002) Crystal Structure and Stability Studies of C77S HiPIP: A Serine Ligated [4Fe-4S] Cluster. *Biochemistry 41*, 1195−1201.
(58) Xiao, Z., Lavery, M. J., Ayhan, M., Scrofani, S. D. B., Wilce, M. C. J., Guss, J. M., Tregloan, P. A., George, G. N., and Wedd, A. G. (1998) The Rubredoxin from *Clostridium pasteurianum*: Mutation of the Iron Cysteinyl Ligands to Serine. Crystal and Molecular Structures of Oxidized and Dithionite-Treated Forms of the Cys42Ser Mutant. *J. Am. Chem. Soc. 120*, 4135−4150.
(59) Hänzelmann, P., Hernández, H. L., Menzel, C., García-Serres, R., Huynh, B. H., Johnson, M. K., Mendel, R. R., and Schindelin, H. (2004) Characterization of MOCS1A, an Oxygen-sensitive Iron-Sulfur

Protein Involved in Human Molybdenum Cofactor Biosynthesis. *J. Biol. Chem. 279*, 34721−34732.
(60) Dailey, H. A., Finnegan, M. G., and Johnson, M. K. (1994) Human ferrochelatase is an iron-sulfur protein. *Biochemistry 33*, 403−407.
(61) Yokoyama, K., Numakura, M., Kudo, F., Ohmori, D., and Eguchi, T. (2007) Characterization and Mechanistic Study of a Radical SAM Dehydrogenase in the Biosynthesis of Butirosin. *J. Am. Chem. Soc. 129*, 15147−15155.
(62) Wong, K. K., Murray, B. W., Lewisch, S. A., Baxter, M. K., Ridky, T. W., Ulissi-DeMario, L., and Kozarich, J. W. (1993) Molecular properties of pyruvate formate-lyase activating enzyme. *Biochemistry 32*, 14102−14110.
(63) McCarty, R. M., Krebs, C., and Bandarian, V. (2013) Spectroscopic, Steady-State Kinetic, and Mechanistic Characterization of the Radical SAM Enzyme QueE, Which Catalyzes a Complex Cyclization Reaction in the Biosynthesis of 7-Deazapurines. *Biochemistry 52*, 188−198.
(64) Amador-Noguez, D., Brasg, I. A., Feng, X.-J., Roquet, N., and Rabinowitz, J. D. (2011) Metabolome Remodeling during the Acidogenic-Solventogenic Transition in *Clostridium acetobutylicum*. *Appl. Environ. Microbiol. 77*, 7984−7997.
(65) Fersht, A. (1985) *Enzyme Structure and Mechanism*, 2nd ed., W. H. Freeman and Co., New York.
(66) Hitchcock, D. I. (1924) The solubility of tyrosine in acid and in alkali. *J. Gen. Physiol. 6*, 747−757.
(67) Cosper, M. M., Jameson, G. N. L., Davydov, R., Eidsness, M. K., Hoffman, B. M., Huynh, B. H., and Johnson, M. K. (2002) The [4Fe-4S]$^{2+}$ Cluster in Reconstituted Biotin Synthase Binds *S*-Adenosyl-l-methionine. *J. Am. Chem. Soc. 124*, 14006−14007.
(68) Chen, D., Walsby, C., Hoffman, B. M., and Frey, P. A. (2003) Coordination and Mechanism of Reversible Cleavage of *S*-Adenosylmethionine by the [4Fe-4S] Center in Lysine 2,3-Aminomutase. *J. Am. Chem. Soc. 125*, 11788−11789.
(69) Dowling, D. P., Vey, J. L., Croft, A. K., and Drennan, C. L. (2012) Structural diversity in the AdoMet radical enzyme superfamily. *Biochim. Biophys. Acta 1824*, 1178−1195.
(70) Challand, M. R., Driesener, R. C., and Roach, P. L. (2011) Radical *S*-adenosylmethionine enzymes: Mechanism, control and function. *Nat. Prod. Rep. 28*, 1696−1721.
(71) Goldman, P. J., Grove, T. L., Sites, L. A., McLaughlin, M. I., Booker, S. J., and Drennan, C. L. (2013) X-ray structure of an AdoMet radical activase reveals an anaerobic solution for formylglycine posttranslational modification. *Proc. Natl. Acad. Sci. U.S.A. 110*, 8519−8524.
(72) Grove, T. L., Ahlum, J. H., Qin, R. M., Lanz, N. D., Radle, M. I., Krebs, C., and Booker, S. J. (2013) Further Characterization of Cys-Type and Ser-Type Anaerobic Sulfatase Maturating Enzymes Suggests a Commonality in the Mechanism of Catalysis. *Biochemistry 52*, 2874−2887.
(73) Grove, T. L., Ahlum, J. H., Sharma, P., Krebs, C., and Booker, S. J. (2010) A Consensus Mechanism for Radical SAM-Dependent Dehydrogenation? BtrN Contains Two [4Fe-4S] Clusters. *Biochemistry 49*, 3783−3785.
(74) Goldman, P. J., Grove, T. L., Booker, S. J., and Drennan, C. L. (2013) X-ray analysis of butirosin biosynthetic enzyme BtrN redefines structural motifs for AdoMet radical chemistry. *Proc. Natl. Acad. Sci. U.S.A. 110*, 15949−15954.
(75) Tureček, F., Carpenter, F. H., Polce, M. J., and Wesdemiotis, C. (1999) Glycyl Radical Is a Stable Species in the Gas Phase. *J. Am. Chem. Soc. 121*, 7955−7956.